Thermodynamics around magnetic phase transitions in alternating double-chain spin systems*

Ding Lin-Jie(丁林杰)†, Zhong Yuan(钟 园), Fan Shuai-Wei(樊帅伟), and Zhu Li-Ya(朱丽娅)

Department of Physics, China Three Gorges University, Yichang 443002, *China*

(Received 21 May 2014; revised manuscript received 26 July 2014; published online 10 October 2014)

The thermodynamics and quantum phase transitions of two typically alternating double-chain systems are investigated by Green's function theory. (i) For the completely antiferromagnetic (AFM) alternating double-chain, the low-temperature antiferromagnetism with gapped behavior is observed, which is in accordance with the experimental result. In a magnetic field, we unveil the ground state phase diagram with zero plateau, 1/2 plateau, and polarized ferromagnetic (FM) phases, as a result of the intra-cluster spin-singlet competition. Furthermore, the Grüneisen ratio is an excellent tool to identify the quantum criticality and testify various quantum phases. (ii) For the antiferromagnetically coupled FM alternating chains, the 1/2 magnetization plateau and double-peak structure of specific heat appear, which are also observed experimentally. Nevertheless, the M–h curve shows an anomalous behavior in an ultra-low field, which is ascribed to the effectively weak Haldane-like state, demonstrated by the two-site entanglement entropy explicitly.

Keywords: thermodynamics, quantum phase transition, double-chain spin system

PACS: 74.25.Bt, 75.30.Kz, 75.10.Pq **DOI:** 10.1088/1674-1056/23/12/127401

1. Introduction

Magnetic materials in the vicinity of a quantum critical point (QCP) have been of particular interest recently, for their properties reflect critical behaviors arising from quantum fluctuations rather than thermal fluctuations, which govern thermal phase transitions.[1–3] Nevertheless, the competition between two different ground states at a QCP gives rise to unusual thermodynamic behaviors.[2–4] In general, a quantum phase transition (QPT) occurs at zero temperature upon tuning a control parameter such as pressure, doping, or magnetic field to a critical value, which is named the balance between the competing ground states.[5–9] Furthermore, at a finite temperature, the underlying QPT manifests unusual sensitivity of thermodynamics with tuning above parameters. Note that, the Grüneisen ratio,

$$\Gamma_r = -\frac{1}{T}\frac{(\partial S/\partial r)_T}{(\partial S/\partial T)_r}$$

with r being the control parameter governing the QPT, is an important tool to identify a QCP.[10,11] If the control parameter to tune the system to the QCP is a magnetic field ($r = h$), the Grüneisen ratio,

$$\Gamma_h = -\frac{1}{T}\frac{(\partial S/\partial h)_T}{(\partial S/\partial T)_h} = -\frac{(\partial M/\partial T)_h}{C_V},$$

which equals the magnetocaloric effect (MCE) with its particularly large value in the vicinity of QCP, is proportional to the cooling rate, namely, the slope of isoentropes in the T–h phase diagram.[12–18] From the above formula, we know that the underlying mechanism leading to an enhanced MCE is related to the large thermal entropy excess that occurs in the vicinity of QCP,[13] where the competing magnetic interactions play a key role. Thus, tuning an external magnetic field and magnetic couplings to select distinct ground states may gain an insight into the QPT as well as the degenerate magnetic ordering that leads to large adiabatic cooling rate.[16]

Low-dimensional magnetic systems with competing interactions are known to present exotic physical properties. One of the most intriguing features is the magnetization plateau.[2,16,17,19] It is interesting to note that Oshikawa *et al.*[20] proposed a necessary condition $n(S-m) = \text{integer}$ for a magnetization plateau appearing in spin chains, with n being the period of the ground state, S the magnitude of spin, and m the magnetization per site. For instance, the two-leg spin-1/2 ladder, which is, indeed, a coupled one-dimensional (1D) spin system, has been widely investigated both experimentally and theoretically for different rung-and-leg interactions. Nevertheless, the predominant rung-singlet is responsible for the gapped behavior and an $M = 0$ plateau.[21–25] However, the 1/2 plateau was not observed due to the absence of competing magnetic interactions along the leg. Quite recently, the quantum behavior of low-dimensional organic molecular-based magnets has been one of the most fascinating topics in condensed matter physics, materials science, and spin chemistry.[24–38] Usually, the magnetic properties are heavily governed by the spatial arrangement of molecular assemblages, in which the intermolecular hydrogen bond-

*Project supported by the National Natural Science Foundation of China (Grant Nos. 11204157, 11174179, and 11247020), the Hubei Provincial Natural Science Foundation, China (Grant No. D20131307), and the China Three Gorges University Project (Grant No. KJ2011B068).

†Corresponding author. E-mail: dinglinjie82@126.com

© 2014 Chinese Physical Society and IOP Publishing Ltd

ing plays an important role in controlling the arrangement of open-shell entities. As a matter of fact, a series of radicals of a nitroxide-based organic molecule have been synthesized experimentally.[26,28–34] Izuoka *et al.*[26] synthesized a molecular complex with alternating biradical and monoradical, where the ferromagnetic (FM) and antiferromagnetic (AFM) couplings compete between each other. Later on, Hosokoshi *et al.*[27] introduced triradical including $S = 1$ and $S = 1/2$ units in a single molecule to synthesize a molecule-based ferrimagnet, in which the competing FM and AFM interactions are responsible for the observed ferrimagnetism. Recently, an organic AFM alternating double-chain compound has been synthesized by Ise *et al.*[29] using four-spin clusters as illustrated in Fig. 1, from which the low-temperature antiferromagnetism was observed. A very recent experimental breakthrough work by Iwase *et al.*[38] who introduced four-spin clusters to synthesize an organic FM alternating double-chain, attracts our attention. In this system, the 1/2 magnetization plateau attributed to the dominant intra-cluster antiferromagnetic coupling, was observed. Hence, the competing magnetic interactions play an important role in determining the magnetic and thermodynamic properties of organic quantum magnets.

Note that the ultra-low temperature (T approaches to 0 K) can hardly be attained in experiment. Thus, the gapped or gapless low-lying excitations were not discovered. Unlike the scenario in the two-leg ladder system[21–23] with rung-singlet being predominant, in alternating double-chain spin systems, the intra-cluster and inter-cluster spin-singlets compete between each other for dominance, which will give rise to various intriguing physical properties in a magnetic field, such as a magnetization plateau associated with QPT and MCE, and a double-peak structure of specific heat. Thus, in order to explore the low-lying excitations and further investigate the field-induced QPT and MCE, the thermodynamics of the alternating double-chain spin system is investigated. The rest of this paper is organized as follows. In Section 2, we present the model Hamiltonian and give an outline of Green's function method. In Section 3, the specific heat, the magnetic susceptibility, the magnetization, the entanglement and thermal entropies, and the Grüneisen ratio are calculated; the field-induced phase diagram is explored; and a comparison with the experimental results is made. Finally, we draw some conclusions from the present studies in Section 4.

2. Model Hamiltonian and theoretical method

For an alternating double-chain spin system as schematically illustrated in Fig. 1, an appropriate spin Hamiltonian reads

$$H = \sum_l \left[J_1 \left(S_{1,l} S_{2,l} + S_{3,l} S_{4,l} \right) + J_2 S_{2,l} S_{3,l} + J_3 \left(S_{2,l} S_{1,l+1} + S_{4,l} S_{3,l+1} \right) \right] - g\mu_B B \sum_l \sum_{i=1}^{4} S_{i,l}^z, \quad (1)$$

where $J_i > 0$ ($J_i < 0$) ($i = 1, 2, 3$) represents AFM (FM) exchange interaction between two contiguous spins. We define the reduced magnetic field $h = g\mu_B B$ (Zeeman energy). By performing Jordan–Wigner (JW) transformation[39–41]

$$\begin{aligned} S_{i,l}^+ &= c_{i,l}^\dagger \, \mathrm{e}^{\mathrm{i}\phi_{i,l}}, \\ \phi_{1,l} &= \pi \left[\sum_{f=1}^{l-1} \sum_{d=1}^{4} n_{d,f} \right], \\ \phi_{i,l} &= \pi \left[\sum_{f=1}^{l-1} \sum_{d=1}^{4} n_{d,f} + \sum_{j=2}^{i} n_{j-1,l} \right], \quad (i = 2,3,4), \\ S_{i,l}^z &= n_{i,l} - 1/2, \end{aligned} \quad (2)$$

with the operator $c_{i,l}^\dagger$ $(c_{i,l})$ creating (annihilating) a spinless fermion at site (i, l) and $n_{i,l} = c_{i,l}^\dagger c_{i,l}$ the corresponding occupation number operator, Hamiltonian (1) becomes

$$\begin{aligned} H = \sum_l \Bigg\{ & \frac{J_1}{2} \left(c_{1,l}^\dagger c_{2,l} + c_{3,l}^\dagger c_{4,l} + \mathrm{H.c} \right) + \frac{J_2}{2} \left(c_{2,l}^\dagger c_{3,l} + \mathrm{H.c} \right) \\ & + \frac{J_3}{2} \left(c_{2,l}^\dagger c_{1,l+1} \, \mathrm{e}^{\mathrm{i}\left(\phi_{2,l} - \phi_{1,l+1}\right)} \right. \\ & \left. + c_{4,l}^\dagger c_{3,l+1} \, \mathrm{e}^{\mathrm{i}\left(\phi_{4,l} - \phi_{3,l+1}\right)} + \mathrm{H.c} \right) \\ & + J_2 \left(n_{2,l} - \frac{1}{2} \right) \left(n_{3,l} - \frac{1}{2} \right) \\ & + J_1 \left[\left(n_{1,l} - \frac{1}{2} \right) \left(n_{2,l} - \frac{1}{2} \right) + \left(n_{3,l} - \frac{1}{2} \right) \left(n_{4,l} - \frac{1}{2} \right) \right] \\ & + J_3 \left[\left(n_{2,l} - \frac{1}{2} \right) \left(n_{1,l+1} - \frac{1}{2} \right) \right. \\ & \left. + \left(n_{4,l} - \frac{1}{2} \right) \left(n_{3,l+1} - \frac{1}{2} \right) \right] \Bigg\} - h \sum_l \sum_{i=1}^{4} \left(n_{i,l} - \frac{1}{2} \right), \end{aligned} \quad (3)$$

which describes a system of interacting spinless fermions with the chosen phases $\phi_{i,l}$ satisfying the spin commutation relation, and is treated within the bond mean-field theory.[6,41,42]

The method we employ is the two-time Green's function theory which has been extensively used to deal with the Heisenberg chain model.[43–46] The retarded Green's function for the JW fermions is defined as

$$\begin{aligned} G_{ij}\left(t - t'\right) &= \left\langle \left\langle a_i(t); b_j^\dagger\left(t'\right) \right\rangle \right\rangle = -\mathrm{i}\theta\left(t - t'\right) \left\langle a_i b_j^\dagger + b_j^\dagger a_i \right\rangle \\ & \left(a, b = c_1, c_2, c_3, c_4\right), \end{aligned} \quad (4)$$

where the subscripts i and j denote lattice sites. After the time Fourier transformation, the Green's function is substituted into the equation of motion,

$$\omega \langle\langle a_i; b_j^\dagger \rangle\rangle = \left\langle \left[a_i, b_j^\dagger \right]_+ \right\rangle + \langle\langle [a_i, H]; b_j^\dagger \rangle\rangle. \quad (5)$$

Using a similar equation of motion and also Eq. (5) for the high-order Green's function $\langle\langle [a_i, H];\ b_j^\dagger \rangle\rangle$, a higher-order

Green's function will appear on the right hand, resulting in an infinite set of coupled equations. In terms of Wick's theorem, we adopt the decoupling scheme[45]

$$\begin{aligned}&\langle\langle c^{\dagger}_{j,m}c_{j,m}c_{i,n};c^{\dagger}_{i,n}\rangle\rangle\\ \approx\ &\langle c^{\dagger}_{j,m}c_{j,m}\rangle\langle\langle c_{i,n};c^{\dagger}_{i,n}\rangle\rangle-\langle c^{\dagger}_{j,m}c_{i,n}\rangle\langle\langle c_{j,m};c^{\dagger}_{i,n}\rangle\rangle.\end{aligned}\tag{6}$$

For further Fourier transformation into k-space, the Green's function can be expressed as

$$G_{ij}=\frac{1}{N}\sum_{k}g(k)\,\mathrm{e}^{\mathrm{i}k\cdot(i-j)}.\tag{7}$$

The integral of the wavevector k extends over the first Brillouin zone. So, the momentum space Green's function $g(k,\omega)$ can be described as a function of wavevector k and the elementary excitation spectrum $\omega=\omega(k)$. According to the standard spectral theorem, the correlation function of the product of fermion operators can be calculated through the corresponding Green's function

$$\begin{aligned}\langle b^{\dagger}_{j}a_{i}\rangle\ =\ &\frac{\mathrm{i}}{2\pi N}\sum_{k}\mathrm{e}^{\mathrm{i}k\cdot(i-j)}\\ &\times\int\frac{\mathrm{d}\omega}{\mathrm{e}^{\beta\omega}+1}\left[g\left(k,\omega+\mathrm{i}0^{+}\right)-g\left(k,\omega-\mathrm{i}0^{+}\right)\right],\end{aligned}\tag{8}$$

where $\beta=1/k_{\mathrm{B}}T$, k_{B} is the Boltzman's constant, and T is the absolute temperature.

Then the average magnetization M per cell and magnetic susceptibility χ are expressed as

$$M=\frac{1}{N}\sum_{l}\sum_{i=1}^{4}\left\langle S^{z}_{l,i}\right\rangle,\ \text{and}\ \chi=\frac{\partial M}{\partial h}.\tag{9}$$

Likewise, the specific heat can be obtained as

$$C_V=\frac{\mathrm{d}E}{\mathrm{d}T}=\frac{\mathrm{d}\langle H\rangle}{\mathrm{d}T}.\tag{10}$$

Thus, we can obtain the thermal entropy,

$$S=\int_{0}^{T}\frac{C_V}{T'}\mathrm{d}T'.\tag{11}$$

The Grüneisen ratio is expressed as

$$\Gamma_h=\frac{1}{T}\left(\frac{\partial T}{\partial h}\right)_{S}=-\frac{1}{T}\frac{(\partial S/\partial h)_T}{(\partial S/\partial T)_h}.\tag{12}$$

Therefore, the above equations can be solved self-consistently. In calculation, an initial state, composed of a set of correlation functions, is substituted into the equations to produce resulting values. The iteration goes on until convergence is reached.

3. Results and discussion

3.1. Completely AFM alternating double-chain

Based on the molecular structure synthesized by Ise *et al*. experimentally,[29] four-spin clusters with intra-cluster couplings (J_1 and J_2) and weak inter-cluster coupling (J_3) being AFM interactions, which form an antiferromagnetically alternating double-chain spin system, are taken into account as illustrated in Fig. 1. For simplicity, we take $k_{\mathrm{B}}=1$ and J_1 as an energy unit ($J_1=1.0$) hereafter, and all other parameters are scaled by J_1. We start our discussion with the analysis of specific heat and magnetic susceptibility for the double-chain spin system in the case of no magnetic field, and the relevant results are plotted in Fig. 2. In order to compare the results of intra-cluster interaction with those of inter-cluster interaction, first, we set $J_2=0.5$. Figure 2(a) shows the temperature dependences of specific heat for different J_3 couplings. One can find that for a small J_3 value, the specific heat decays exponentially to zero as $T\to 0$ after a round maximum due to the existence of a finite energy gap between the ground state and the excitation state. It is clearly manifested by $\ln(C_V)$–$1/T$ curve at low temperature in the inset, where $\ln(C_V)$ behaves linearly with $1/T$, giving rise to $C_V\propto\mathrm{e}^{-\Delta/k_{\mathrm{B}}T}$, of which the slope reflects the magnitude of energy gap ($-\Delta$).[23] By increasing the J_3 value, the single peak moves towards a high temperature with its maximum suppressed for $J_3<1.0$, beyond which its maximum is enhanced. It is due to the combination of energy variation and energy gap.[7] The gapped low-lying excitations can also be identified by the temperature dependence of magnetic susceptibility as shown in Fig. 2(c). Likewise, the susceptibility is exponentially activated at an ultra-low temperature after a round peak, which shifts towards a lower temperature with its maximum decreasing as J_3 increases for $J_3<1.0$, which is attributed to the dominant J_1-singlets. For $J_3>1.0$ the scenario is reversed: the round peak moves towards a higher temperature region, which is due to the dominant J_3-singlets. Wondrously, as J_3 approaches to 1.0, a shoulder appears at low temperature, reflecting the uniform antiferromagnetism along the chain. It should be emphasized that the low-energy properties of the spin system are governed mainly by the intra-cluster interactions. In other words, the intra-cluster singlet-dimer is more robust than the inter-cluster coupling. Thus, the ground state consists of essentially coupled dimers or singlet-dimer recombination. In order to make a comparison with the experimental observation, herein, the weak inter-cluster coupling (J_3) is considered and set to be 0.1, so that the competition between different intra-cluster couplings (J_1 and J_2) is responsible for the rich thermodynamic phenomena. Figure 2(b) shows the temperature dependence of specific heat, which decays exponentially to zero as $T\to 0$ after a round maximum for $J_2<1.0$, indicating a gapped low-lying excitation. In this case, the J_1-singlet predominates over the system with a large

gap. After J_2 exceeds J_1, the single peak of specific heat splits into two peaks in which its low-temperature peak moves towards a lower temperature region as J_2 increases, therefore the J_2-singlet becomes more and more dominant. Meanwhile, we plot the temperature dependence of the magnetic susceptibility in Fig. 2(d). It is clearly shown that as $T \to 0$, the susceptibility goes exponentially to zero after a round maximum, indicating a gapped behavior. Though the round peak shifts towards low temperature with J_2 ascending, its maximum is suppressed for $J_2 < 1.0$ while enhanced for $J_2 > 1.0$. The former is attributed to the dominated J_1-singlet, while the latter is due to the J_2-singlet. Furthermore, we also calculate the susceptibility multiplied by temperature that decreases continuously upon cooling (see the left inset), reflecting the low-temperature antiferromagnetism of the system, which is in accordance with the experimental results and illustrated in the right inset. Besides, we plot χ^{-1} versus temperature in the left inset of Fig. 2(d), where the extrapolation from the high temperature portion of the curve gives a small negative Weiss temperature, indicating the low-temperature antiferromagnetism of the system according to Curie–Weiss law. Nevertheless, at an ultra-low temperature, χ^{-1} diverges as $T \to 0$, of which the behavior was observed in the ladder compound Cu(2,3-dimethylpyrazine)Br_2,[47] indicating the gapped spin liquid ground state.

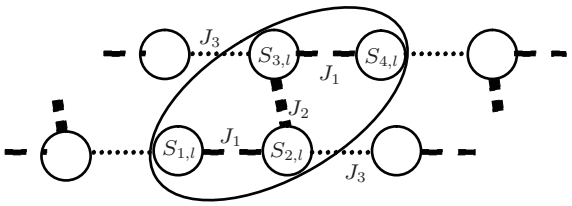


Fig. 1. Schematic diagram of a molecular alternating double-chain spin system. The empty circle represents spin-1/2. J_i ($i = 1, 2, 3$) are the intra-cluster and inter-cluster interactions, respectively.

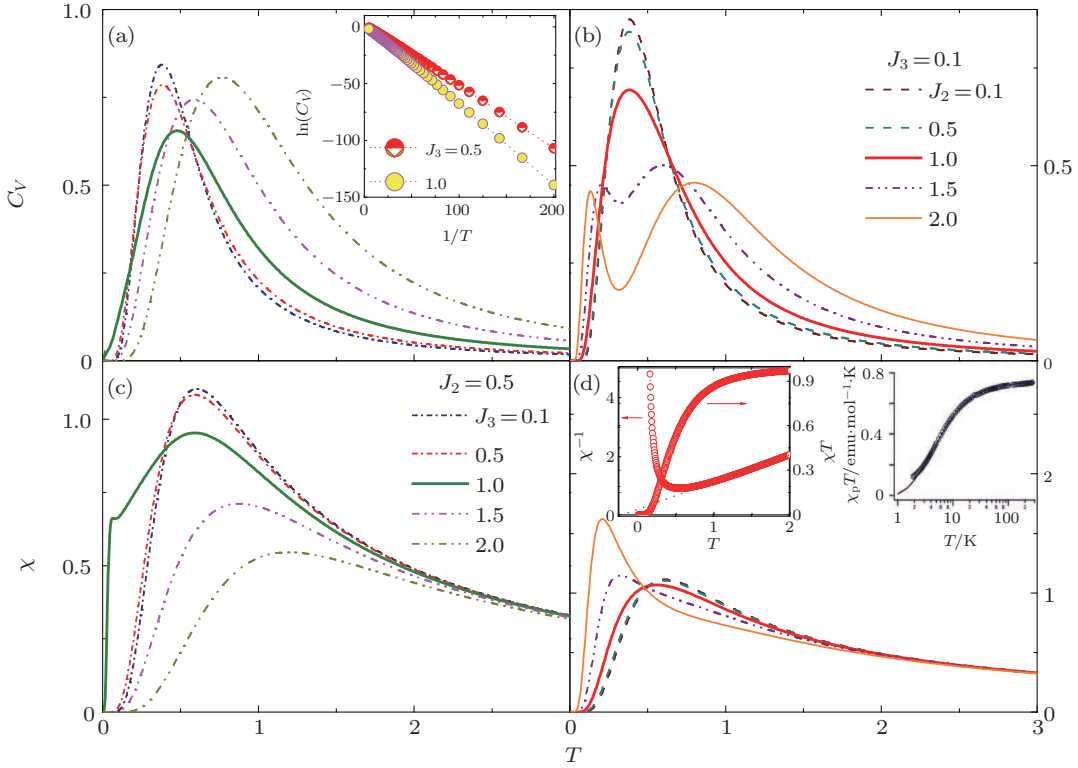


Fig. 2. (color online) The temperature dependences of specific heat for different J_3 couplings with $J_2 = 0.5$ (a) and for different J_2 couplings with $J_3 = 0.1$ (b). The inset in panel (a) shows the logarithm of specific heat versus $1/T$. The temperature dependences of susceptibility in panels (c) and (d) for the parameters corresponding to those in panels (a) and (b), respectively. The left inset in panel (d) is the temperature multiplied by susceptibility and χ^{-1} as a function of temperature, compared with the experimental measurement cited from Ref. [29] (see the right inset).

As a magnetic field is turned on, the striking features are found. Figure 3(a) presents the (J_2, h) phase diagram with $J_3 = 0.1$. One can find $M = 0$ plateau, 1/2 plateau, and polarized FM phases separated by two critical lines (h_c and h_s) denoting the first order QPTs, which are explicitly evident by the field dependence of magnetization in Figs. 3(b)–3(d). It is also shown that there is a tricritical point $J_{2c} = 0.25$. For weak J_2 coupling ($J_2 < J_{2c}$) as plotted in Fig. 3(b), the M–h curve presents an $M = 0$ plateau, of which the occurrence implies that half the spins connected by J_1-form spin-singlet pairs with a dimer gap. It is confirmed by the zero value of the magnetic moment of each sublattice (see the left in-

set). Thus, the $M = 0$ plateau results from the J_1-singlet. It is also clearly demonstrated by the two-site entanglement entropy defined as $E_{i,j} = -\mathrm{Tr}\,[\rho_{i,j} \ln(\rho_{i,j})]$,[48] where the two-site reduced density matrix $\rho_{i,j}$ consists of correlation functions as shown in the right inset. Herein, we define E_{J1} and E_{J2} as the entanglements for the subsystem (dimer connected by J_1 and J_2) with the rest of the system, respectively. It is shown that the entanglement plateau corresponds to the field region where the magnetization plateau occurs. In the zero plateau region, $E_{J1} < E_{J2}$, suggesting that the J_1-singlet pairs predominate over the system. As h ascends, M jumps into its saturation value, as a result of the field-induced splitting from singlet state to quintet state. Figure 3(c) shows that for intermediate J_2 coupling ($J_2 = J_1$), the $M = 0$ plateau is still maintained, in which the J_1-singlet predominates over the system somewhat, which is confirmed by zero magnetic moments of each sublattice (see the upper inset). By further increasing h, M suddenly enters into a 1/2-plateau, which is attributed to the combination of J_1- and J_2-singlets along the chain. It can be explained qualitatively as follows. In a strong field, the J_1-singlets are destroyed with equal probability, resulting in the spin-singlet recombination because of the comparative J_1 and J_2 values. It is clearly testified in the upper inset of Fig. 3(c), where both the magnetic moments of each sublattice contribute to the 1/2-plateau, yet $\langle S_{1,4}\rangle$ wins over $\langle S_{2,3}\rangle$. The lower inset of Fig. 3(c) also presents the entanglement entropy versus h, in which E_{J1} and E_{J2} show almost the same response to the field, implying that the coexistence of J_1- and J_2-singlets are responsible for the intermediate 1/2-plateau. For large J_2 value ($J_2 > J_1$), figure 3(d) shows that the $M = 0$ plateau narrows, which is ascribed to the coexistence of J_1-singlet and an effectively weak inter-chain singlet connected by sublattice S_1 and S_4 with J_2-singlet imbedded therein. It is illustrated by $E_{J1} = E_{J2}$ in the low field (see the lower inset).[49] Further increasing h, the J_1-singlets and effective spin singlets are destroyed, bringing to the J_2-singlets responsible for the 1/2-plateau. It is confirmed by the dominant contribution of the magnetic moment of $\langle S_{1,4}\rangle$ to the 1/2-plateau (see the upper inset). From the lower inset of Fig. 3(d), one can see $E_{J2} < E_{J1}$ in the same field region, implying that the J_2-singlet predominates. In this case, the QPT is attributed to the field-induced splitting of states, which yields a level crossing of the singlet ground state with the triplet state and a second level crossing of the triplet state with the quintet state sequentially.

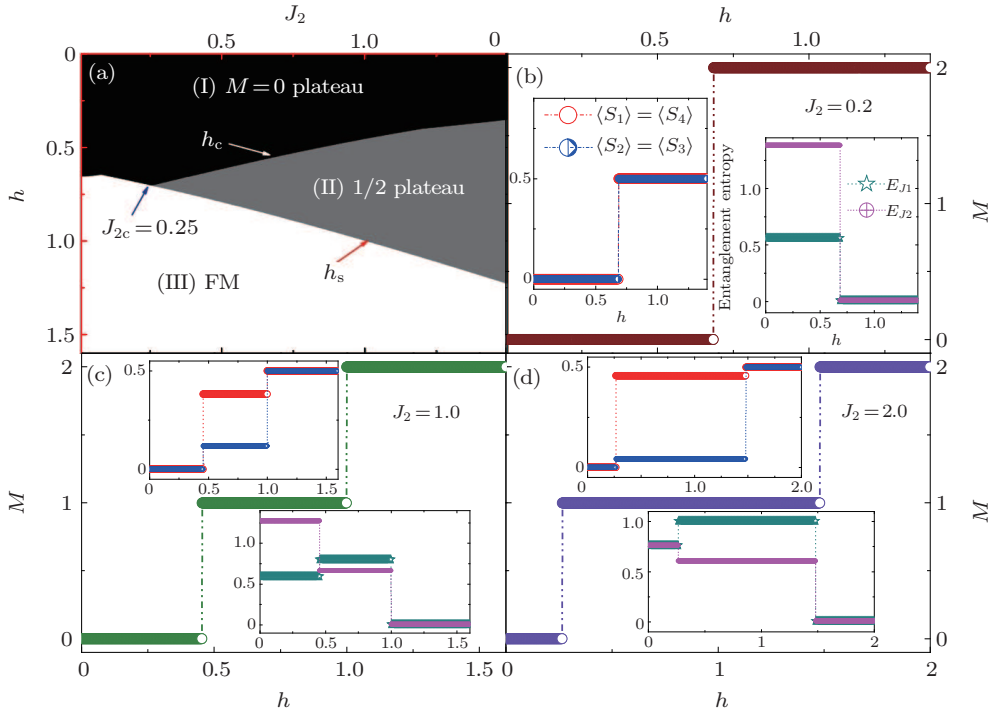


Fig. 3. (color online) (a) J_2–h phase diagram for $J_3 = 0.1$, showing the zero plateau, 1/2-plateau, and polarized FM phases. Panels (b), (c), and (d) show magnetization curves for different J_2 values to manifest the phase diagram. The insets show the field dependences of sublattice magnetization and two-site entanglement entropy, respectively.

To gain further insight into the study of field-induced QPTs, we investigate the thermal entropy S values for $J_2 = 1.0$ and $J_3 = 0.1$. We are aware that there has been calculation of the thermal entropy and accordingly the isoentropes for a one-dimensional spin system in a magnetic field to demonstrate the quantum criticality.[12–17] Figure 4(a) shows the isoentropes in the h–T plane. The QPTs at h_c and h_s are demonstrated by the deeps of the isoentropes as a function of h, or equivalently the sharp maxima of the thermal entropy at ultra-low temperature (see Fig. 4(b)). The accumulation of thermal entropy close to

QCPs indicates that what is maximally undetermined in the system is which ground state should be chosen. Besides, the field dependence of Grüneisen ratio Γ_h for $T = 0.005$ is plotted in Fig. 4(c), which presents the very sharp and pronounced positive peaks and negative valleys at the critical fields. The argumentation of Garst and Rosch[10] shows that the Grüneisen ratio Γ_h, which is proportional to the magnetic cooling rate, displays a characteristic divergent behavior close to the QCP and changes sign as the field crosses it. Here, the large positive Γ_h values indicate that a pronounced cooling effect is obtained via adiabatic demagnetization in a corresponding h–T range. Besides, the Grüneisen parameter Γ_h is also a good quantity to testify various quantum phases explicitly as shown in Fig. 4(d). One can find that as the temperature ascends, Γ_h increases monotonically with its sign changing for $h < h_c$. In contrast, Γ_h is positive and decreases monotonically in the FM phase with temperature ascending. Unlike the above two phases, Γ_h shows an upturn in the 1/2-plateau state.

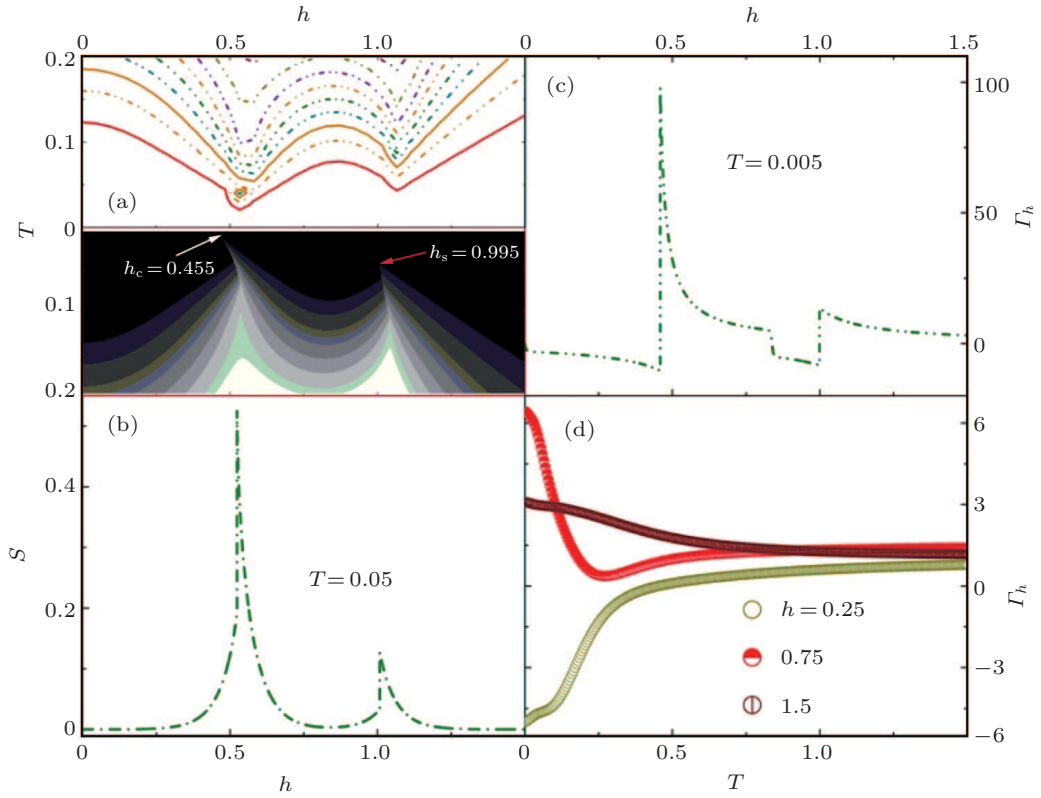


Fig. 4. (color online) For $J_2 = 1.0$ and $J_3 = 0.1$, (a) the isoentropes (upper panel) and $S(T, h)$ (lower panel); (b) the field dependence of thermal entropy with $T = 0.05$; (c) the field dependences of Grüneisen ratio; and (d) the Grüneisen ratio as a function of temperature for different fields.

3.2. Antiferromagnetically coupled FM alternating double-chain

Quite recently, according to the experimental report by Iwase *et al.*,[38] we know that the system consists of antiferromagnetically coupled FM alternating chains, namely, J_2 is as an AFM coupling, while J_1 and J_3 are FM couplings. In order to compare our results with the experimental results and quantum Monte Carlo (QMC) simulation, we set $J_1/k_B = -28$ K, $J_2 = -1.5J_1$, and $J_3 = 0.25J_1$.[38] We plot the field dependence of magnetization under different temperatures in Fig. 5(a). It clearly demonstrates that we obtain a 1/2-magnetization plateau with two critical fields h_c (=0.216, i.e. $B_c = h_c|J_1|/g\mu_B = 4.5$ T, marking the continuous QPT) and h_s (=1.205, i.e. $B_s = h_s|J_1|/g\mu_B = 25.1$ T, denoting the first order QPT, namely, a steplike behavior predicted by Iwase *et al.*), which coincide with the experimental results 5 T and 23.5 T, respectively. As the temperature ascends, the magnetization plateau is smeared out due to the strong thermal fluctuations. Furthermore, the differential curve $(\mathrm{d}M/\mathrm{d}h)$ shows a peak at about $h = h_s$ and a shoulder in a low field region as indicated in Fig. 5(b). Especially, upon cooling, a noticeable spin-flop-like behavior appears at $h_{SF} = 0.034$ ($B_{SF} = h_{SF}|J_1|/g\mu_B = 0.7$ T, which is bigger than the experimental data 0.1 T to some extent, however, its small value is responsible for the too small energy gap to be detected), where the field derivative of magnetization displays a distinct peak as shown in the lower inset of Fig. 5(a). On the whole, all these behaviors are consistent with the experimental observations, which are illustrated in the upper inset of Fig. 5(a). As is well known, the spin–orbital coupling is rather weak in organic molecular magnets so that one can ignore the magnetic anisotropy. Therefore, we are apt to believe that the Haldane-like state[50,51] is responsible for

the spin-flop-like behavior. In a low field, the J_1-triplet predominates over the system rather, forming an effective weak AFM spin-1 dimer, which should present a very small Haldane gap that can be washed out easily by thermal fluctuations even at an ultra-low temperature. It is evidenced by the field dependence of entanglement entropy (see the left inset of Fig. 5(b)), where E_{J1} shows a round maximum at about h_{SF}, indicating that the J_1-triplet predominates for $h < h_{SF}$, beyond which the J_2-singlet predominates. In this case, the J_1-triplets are delocalized by increasing h gradually, accompanied by J_2-singlet recombination, leading to a transition from a Haldan-like state to Luttinger-like liquid. Correspondingly, the field dependence of E_{J1} for stronger J_2 coupling is plotted in the right inset of Fig. 5(b), which shows a shoulder dropping continuously with h increasing, implying that the dominant J_2-singlet is responsible for the gapless low-lying excitation even for $h = 0$. In addition, in order to identify the QCP, we also investigate the thermal entropy S, and the results are shown in Fig. 5(c). The QPTs at h_{SF}, h_c, and h_s are demonstrated by the minima of the isentropes each as a function of h, or equivalently the maxima of the thermal entropies at an ultra-low temperature. Meanwhile, the developing divergence of Grüneisen ratio Γ_h combined with a sign change gives rise to a strong signature of the MCE at the critical fields, as illustrated in Fig. 5(d).

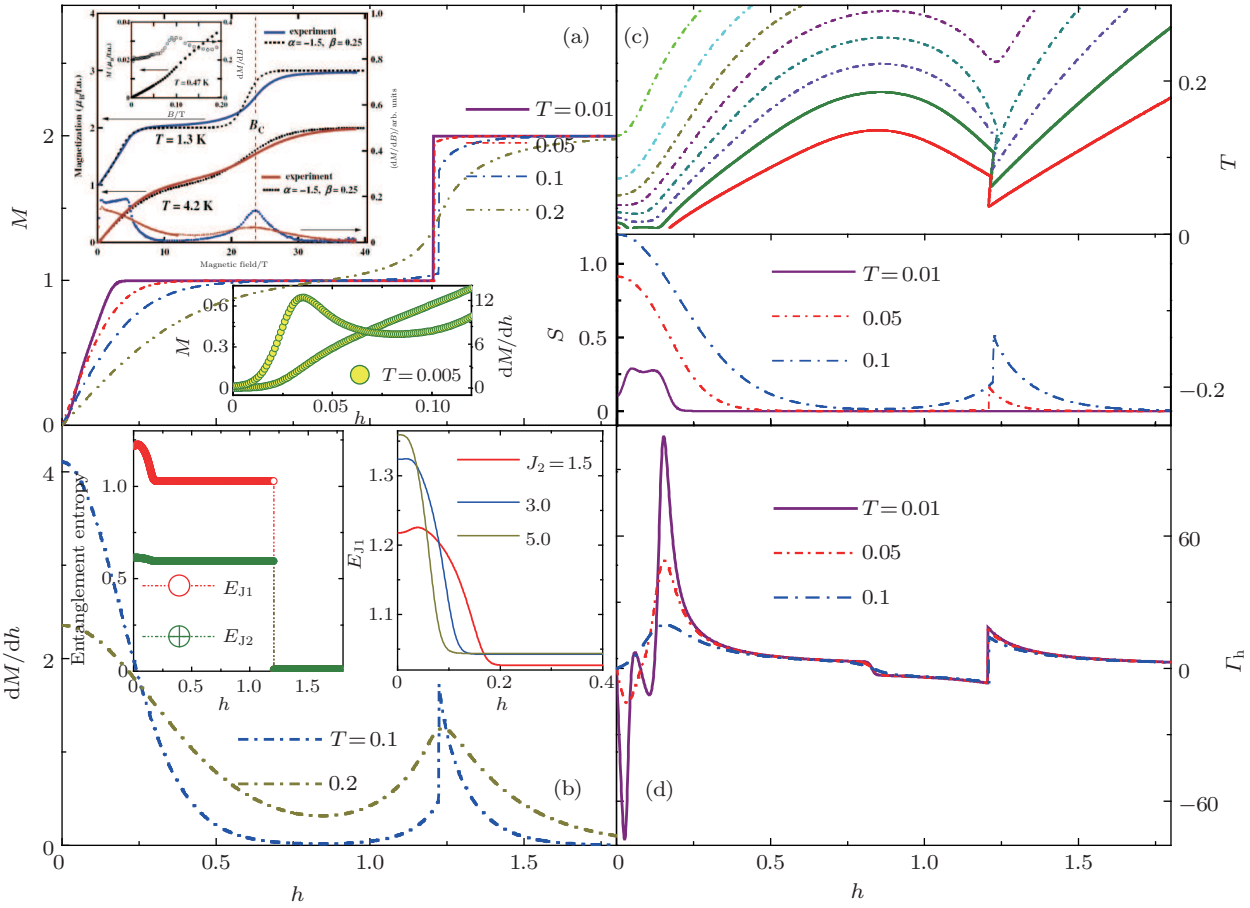


Fig. 5. (color online) (a) The field dependences of magnetization under different temperatures for $J_2 = 1.5$ and $J_3 = -0.25$, the lower inset shows the low-field M–h curve and its derivation, compared with the experimental results in the upper inset cited from Ref. [38]. (b) The first derivations of magnetization M against h ($\mathrm{d}M/\mathrm{d}h$) for $T = 0.1$ and 0.2. The inset shows the two-site entanglement entropy against h. (c) The isoentropes in (T, h) parameter space in the upper panel and the thermal entropy versus h under low temperatures in the lower panel. (d) The variation of Grüneisen parameter Γ_h with field at low temperatures.

Accordingly, in different fields, the thermodynamics behave differently. In Fig. 6(a) for $h = 0$, the temperature dependence of specific heat displays a double-peak structure and almost T-linear relation as $T \to 0$ because the very small energy gap was washed out easily even at ultra-low temperatures. The low temperature peak was also observed experimentally.[38] As h increases, the system enters into the Luttinger liquid state ($h < h_c$), where the double-peak structure is still held, with a shoulder occurring as $T \to 0$. As h exceeds but is near to h_c as shown in Fig. 6(b), although the double-peak structure is still held there, the specific heat decays exponentially as T goes to zero due to an energy gap opened up by the field. Never-

theless, the low-temperature reflects the importance of critical fluctuations. Further increasing h, the double-peak merges into a single one, which moves towards the low temperature region with its maximum enhanced for $h < (h_c + h_s)/2$. In the fermion mapping, we can obtain two positive-energy excitations (fermion excitations) and two negative-energy excitations (hole excitations).[7] This shift is ascribed to the fermion excitations whose gap decreases with h ascending. After h exceeds $(h_c + h_s)/2$, the single peak shifts to a high temperature with its maximum suppressed, which is attributed to the hole excitations whose gap increases (see Fig. 6(c)). As $h = h_s$, an additional low-temperature peak occurs as a result of critical fluctuations. For the field beyond h_s, the specific heat is exponentially activated as T goes to zero after a round peak which shifts towards a high temperature due to the energy gap augmenting with h increasing as indicated in Fig. 6(d).

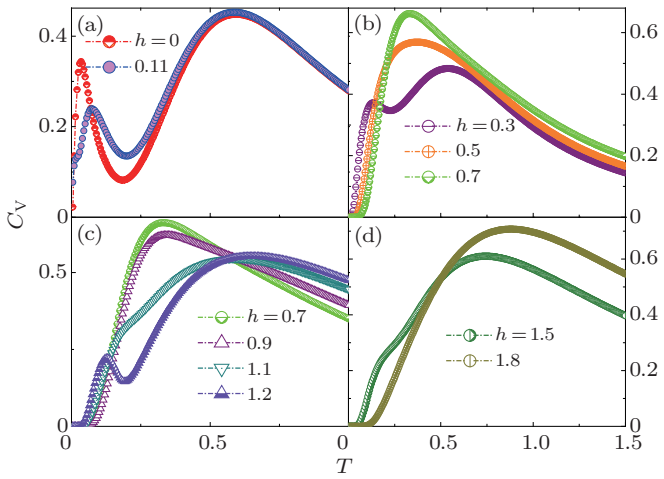


Fig. 6. (color online) Variations of specific heat with temperature under fields of (a) $h < h_c$; (b) $h_c < h < (h_c + h_s)/2$; (c) $(h_c + h_s)/2 < h < h_s$; and (d) $h > h_s$.

4. Conclusions

In this paper, based on an organic alternating double-chain system synthesized using four-spin clusters experimentally, the thermodynamics and QPTs of two typically physical topics are investigated in detail by Green's function theory. For the completely AFM alternating double-chain system, our results show that the system presents low-temperature antiferromagnetism with gapped low-lying excitation, which is consistent with the experimental observation. When the magnetic field is turned on, the ground state phase diagram shows the zero plateau, 1/2-plateau, and polarized FM phases with the occurrence of first order QPTs, which are explicitly confirmed by the field dependence of magnetization. It is found that the emergence of zero and 1/2 plateaus results from the competition between intra-cluster J_1- and J_2-singlets. For weak J_2 coupling, the magnetization presents only a zero plateau attributed to the dominant J_1-singlet. For intermediate J_2 coupling ($J_2 \sim J_1$), it presents a zero plateau attributed to the J_1-singlet, and a 1/2-plateau, in which the J_1- and J_2-singlets coexist. As J_2 is large, the zero and 1/2 plateaus still exist. Nevertheless, the former is ascribed to the combination of the J_1-singlet and effective weak inter-chain singlet assembled by sublattices S_1 and S_4 after the J_2-singlet formation, while the latter corresponds to the predominant J_2-singlet. Besides, the QPTs are demonstrated by the deeps of isoentropes each as a function of h, or equivalently the sharp maxima of thermal entropies at an ultra-low temperature. It is interesting to note that the Grüneisen ratio proportional to the magnetic cooling rate is a useful tool to identify QCPs and testify various quantum phases.

For the antiferromagnetically coupled FM alternating chains as the model of organic compound m-Ph-V_2, it is shown that the field dependence of magnetization presents a 1/2-plateau attributed to the dominant J_2-singlet with two critical fields $B_c = 4.5$ T and $B_s = 25.1$ T, where the step-like QPT occurs, corresponding to the analysis by Iwase *et al*.[38] Our results are in agreement with the experimental observation and QMC simulation. The specific heat displays a double-peak structure. The low temperature one was also observed in experiment. Nevertheless, the M–h curve shows a spin-flop-like behavior in an ultra-low field, which was also observed experimentally. This anomalous behavior is further detected by the field dependence of thermal entropy and the Grüneisen ratio at an ultra-low temperature, and it is ascribed, we believe, to the effective weak Haldane-like state, demonstrated by the two-site entanglement entropy explicitly.

References

[1] Sachdev S 2000 *Science* **288** 475
[2] Kikuchi H, Fujii Y, Chiba M, Mitsudo S, Idehara T, Tonegawa T, Okamoto K, Sakai T, Kuwai T and Ohta H 2005 *Phys. Rev. Lett.* **94** 227201
[3] Wolfa B, Tsuia Y, Jaiswal-Nagara D, Tutscha U, Honeckerb A, Remović-Langera K, Hofmanna G, Prokofievc A, Assmusa W, Donathd G and Langa M 2011 *Proc. Natl. Acad. Sci. USA* **108** 6862
[4] Liu W J, Xin Z H, Chen S L and Zhang C Y 2013 *Chin. Phys. B* **22** 027501
[5] Carr L D 2011 *Understanding Quantum Phase Transitions* (CRC Press, Taylor and Francis Group, LLC)
[6] Azzouz M 2008 *Phys. Rev. B* **78** 014421
[7] Gong S S, Gao S and Su G 2009 *Phys. Rev. B* **80** 014413
[8] Chen S R, Xia Y J and Man Z X 2010 *Chin. Phys. B* **19** 050304
[9] Tan X D, Jin B Q and Gao W 2013 *Chin. Phys. B* **22** 020308
[10] Garst M and Rosch A 2005 *Phys. Rev. B* **72** 205129
[11] Meingast C, Hardy F, Heid R, Adelmann P, Böhmer A, Burger P, Ernst D, Fromknecht R, Schweiss P and Wolf T 2012 *Phys. Rev. Lett.* **108** 177004
[12] Trippe C, Honecker A, Klümper A and Ohanyan V 2010 *Phys. Rev. B* **81** 054402
[13] Qi Y, Du A and Ma Y 2012 *Phys. Lett. A* **377** 27
[14] Jafari R 2012 *Eur. Phys. J. B* **85** 167
[15] Topilko M, Krokhmalskii T, Derzhko O and Ohanyan V 2012 *Eur. Phys. J. B* **85** 278
[16] Ohanyan V and Honecker A 2012 *Phys. Rev. B* **86** 054412
[17] Boyarchemkov A S, Bostrem I G and Ovchinnikov A S 2007 *Phys. Rev. B* **76** 224410
[18] Pereira M S S, de Moura F A B F and Lyra M L 2009 *Phys. Rev. B* **79** 054427
[19] Totsuka K 1997 *Phys. Rev. B* **57** 3454

[20] Oshikawa M, Yamanaka M and Affleck I 1997 *Phys. Rev. Lett.* **78** 1984

[21] Rüegg Ch, Kiefer K, Thielemann B, McMorrow D F, Zapf V, Normand B, Zvonarev M B, Bouillot P, Kollath C, Giamarchi T, Capponi S, Poilblanc D, Biner D and Krämer K W 2008 *Phys. Rev. Lett.* **101** 247202

[22] Ding L J, Yao K L and Fu H H 2010 *ChemPhysChem* **11** 3291

[23] Hong T, Kim Y H, Hotta C, Takano Y, Tremelling G, Turnbull M M, Landee C P, Kang H J, Christensen N B, Lefmann K, Schmidt K P, Uhrig G S and Broholm C 2010 *Phys. Rev. Lett.* **105** 137207

[24] Yamaguchi H, Iwase K, Ono T, Shimokawa T, Nakano H, Shimura Y, Kase N, Kittaka S, Sakakibara T, Kawakami T and Hosokoshi Y 2013 *Phys. Rev. Lett.* **110** 157205

[25] Yamaguchi H, Miyagai H, Shimokawa T, Iwase K, Ono T, Kono Y, Kase N, Araki K, Kittaka S, Sakakibara T, Kawakami T, Okunishi K and Hosokoshi Y 2014 *J. Phys. Soc. Jpn.* arXiv: 1402.2743v1

[26] Iruoka A, Fukada M, Kumai R, Itakura M, Hikami S and Sugawara T 1994 *J. Am. Chem. Soc.* **116** 2609

[27] Shiomi D, Kanaya T, Sato K, Mito M, Takeda K and Takui T 2001 *J. Am. Chem. Soc.* **123** 11823

[28] Hayakawa K, Shiomi D, Ise T, Sato K and Takui T 2006 *J. Mater. Chem.* **16** 4146

[29] Ise T, Shiomi D, Sato K and Takui T 2006 *Chem. Commun.* **46** 4832

[30] Maekawa K, Shiomi D, Ise T, Sato K and Takui T 2007 *Org. Biomol. Chem.* **5** 1641

[31] Gilroy J B, McKinnon S D J, Kennepohl P, Zsombor M S, Ferguson M J, Thompson L K and Hicks R G 2007 *J. Org. Chem.* **72** 8062

[32] Zoppellaro G, Geies A, Andersson K K, Enkelmann V and Baumgarten M 2008 *Eur. J. Org. Chem.* 1431

[33] Tanaka H, Shiomi D, Suzuki S, Kozaki M, Okada K, Sato K and Takui T 2010 *CrystEngComm* **12** 526

[34] Hui P, Arif M K and Chandrasekar R 2012 *Org. Biomol. Chem.* **10** 2439

[35] Gao Y, Liu C G and Jiang Y S 2002 *J. Phys. Chem. A* **106** 2592

[36] Zhu Y Y, Cui C, Li N, Wang B W, Wang Z M and Gao S 2013 *Eur. J. Inorg. Chem.* 3101

[37] Zhao Y, Li W, Xi B, Ran S J, Zhu Y Y, Wang B W, Gao S and Su G 2013 *Europhys. Lett.* **104** 57009

[38] Iwase K, Yamaguchi H, Ono T, Shimokawa T, Nakano H, Matsuo A, Kindo K, Nojiri H and Hosokoshi Y 2013 *J. Phys. Soc. Jpn.* **82** 074719

[39] Jordan P and Wigner E 1928 *Z. Phys.* **47** 631

[40] Lieb E, Schultz T and Mattis D 1961 *Ann. Phys.* **16** 407

[41] Azzouz M 1993 *Phys. Rev. B* **48** 6136

[42] Azzouz M 2007 *Phys. Rev. B* **76** 064419

[43] Tyablikov S V 1967 *Methods in the Quantum Theory of Magnetism* (New York: Plenum)

[44] Callen H B 1963 *Phys. Rev.* **130** 890

[45] de Lima J P and Goncalves L L 1999 *J. Magn. Magn. Mater.* **206** 135

[46] Fröbrich P and Kuntz P J 2006 *Phys. Rep.* **432** 223

[47] Wells B M, Landee C P, Turnbull M M, Awwadi F F and Twamley B 2005 *J. Mol. Cat. A: Chem.* **228** 117

[48] Li Y C and Li S S 2008 *Phys. Rev. B* **78** 184412

[49] Yamaguchi H, Okubo T, Iwase K, Ono T, Kono Y, Kittaka S, Sakakibara T, Matsuo A, Kindo K and Hosokoshi Y 2013 *Phys. Rev. B* **88** 174410

[50] Haldane F D M 1983 *Phys. Rev. Lett.* **50** 1153

[51] Date M and Kindo K 1990 *Phys. Rev. Lett.* **65** 1659